

Increases in Mitral Leaflet Radii of Curvature with Chronic Ischemic Mitral Regurgitation

Frederick A. Tibayan¹, Filiberto Rodriguez¹, Frank Langer¹, Mary K. Zasio¹, Lynn Bailey², David Liang², George T. Daughters^{1,3}, Matts Karlsson³, Neil B. Ingels, Jr.^{1,3}, D. Craig Miller¹

¹Department of Cardiovascular and Thoracic Surgery, ²Division of Cardiovascular Medicine, Stanford University School of Medicine, Stanford, California, ³Laboratory of Cardiovascular Physiology and Biophysics, Research Institute of the Palo Alto Medical Foundation, Palo Alto, California, USA

Background and aim of the study: Leaflet curvature is a primary determinant of leaflet stress, but no quantitative in-vivo leaflet curvature data exist. Chronic ischemic mitral regurgitation (CIMR) is associated with remodeling of the valvular-ventricular complex. It was hypothesized that leaflet radii of curvature (ROC) would change with such remodeling.

Methods: Twelve sheep had placement of radiopaque markers on the anterior (APM) and posterior (PPM) papillary muscles, mitral annulus, and anterior (AL) and posterior leaflet (PL) midlines. After 8 ± 2 days, videofluoroscopy provided baseline 3-D marker data prior to creating inferior myocardial infarction (MI) by snare occlusion of the obtuse marginal coronary arteries. After 7 ± 1 weeks, the animals were re-studied; 3-D marker coordinates were used to determine end-systolic leaflet ROC, leaflet length, annular septal-lateral diameter, and the distance of each papillary muscle to the mid-septal annulus and each commissure.

Results: Before and after CIMR, the AL had compound curvature, and CIMR increased ROC of both

curves (proximal ROC 1.27 ± 0.59 to 1.38 ± 0.60 cm ($p < 0.05$); distal ROC 1.41 ± 0.61 to 2.60 ± 1.52 cm ($p < 0.05$)). The PL ROC also increased with CIMR (from 2.01 ± 1.40 to 3.46 ± 3.93) ($p < 0.05$). Multiple regression analysis determined that annular septal-lateral diameter (proximal AL and distal AL), distance from the APM to anterior commissure (distal AL), and PPM to mid-septal annulus (PL) were independent predictors of leaflet ROC.

Conclusion: CIMR increased ROC of both the AL and PL. Leaflet extension may be a compensatory mechanism to minimize the regurgitant orifice, but the attendant increase in ROC will tend to augment leaflet stress. Annular and subvalvular geometry both affect leaflet curvature, and should be considered during mitral repair. These novel quantitative in-vivo data are now available for modification of finite element models, and for comparison to finite element model output.

The Journal of Heart Valve Disease 2004;13:772-778

Mitral leaflet shape is a fundamental determinant of leaflet function. Mathematical models of the mitral valve relate curvature of the leaflet to leaflet stress by Laplace's law (1-6). In disease, alterations in leaflet shape (and, subsequently, leaflet stress) induced by left ventricular remodeling lead to compensatory leaflet thickening that may hinder normal valve closure or even compromise the potential for repair (7,8). Echocardiographic (9) and cinefluoroscopic (10,11) studies have noted the direction of curvatures in the

closed valve, but no leaflet radii of curvature (ROC) quantitative data exist. Further, the effects of ventricular remodeling on leaflet curvature are unknown.

Chronic ischemic mitral regurgitation (CIMR) causes global ventricular dilation and distortions of the annulus and papillary muscles (12-14). Given the complex interdependence of the mitral apparatus, these changes in annular and subvalvular geometry may alter leaflet shape (15). In the present study, mitral leaflet shape was quantified, and it was hypothesized that remodeling associated with CIMR would increase leaflet ROC.

Materials and methods

Surgical preparation

Forty-three Dorsett hybrid sheep (mean \pm SD body weight 71 ± 5 kg) were premedicated with ketamine

Presented at the Second Biennial Meeting of the Society for Heart Valve Disease, 28th June-1st July 2003, Palais des Congrès, Paris, France

Address for correspondence:

D. Craig Miller MD, Department of Cardiothoracic Surgery, Falk Cardiovascular Research Center, Stanford University School of Medicine, Stanford, CA 94305-5247, USA
e-mail: dcm@stanford.edu

(25 mg/kg, intramuscular), and anesthesia was induced with sodium thiopental (6.8 mg/kg, i.v.) and maintained with inhalational isoflurane (1-2.5%). Through a left thoracotomy, eight tantalum myocardial markers (#2-9) were inserted in the left ventricular epicardial layer along four equally spaced longitudinal meridians, with one marker at the left ventricular apex (#1; Fig. 1). Prolene 2-0 sutures were passed loosely around the one, two (or occasionally three) obtuse marginal branches of the left circumflex coronary artery located between the posterior vein of the left ventricle and the middle cardiac vein, and loosely snared using the method of Llaneras et al. (16). After commencing cardiopulmonary bypass, tantalum markers were placed at the tips of both the anterior and posterior papillary muscles (APM #12 and PPM #13), and eight markers were sutured around the circumference of the mitral annulus (MA) (one near each commissure (#16, #20), and three along the septal (#15, 21, 22) and lateral (#17, 18, 19) annulus (Fig. 1). Miniature gold markers were sutured along the midlines of the anterior (#23, 24, 25) and posterior (#26, 27) leaflets. A micromanometer pressure transducer (PA4.5-X6; Konigsberg Instruments, Inc., Pasadena, CA, USA) was placed in the left ventricular chamber

through the apex. Postoperatively, 11 animals died from respiratory complications.

Experimental protocol

After 8 ± 2 days, each animal was taken to the cardiac catheterization laboratory, sedated with ketamine (1-4 mg/kg/h, i.v. infusion) and diazepam (5 mg, i.v.), intubated, mechanically ventilated, and maintained with inhalational isoflurane (1-2.5%). Transesophageal echocardiography (TEE) and coronary angiography were performed, and baseline videofluoroscopic marker and hemodynamic data acquired. After premedication with lidocaine (100 mg, i.v.), bretylium (75 mg, i.v.), and magnesium (3 g, i.v.), the coronary artery snares were tightened, and complete occlusion of the selected vessels was verified by angiography. An epinephrine (adrenaline) drip was titrated to maintain the coronary perfusion pressure (aortic diastolic pressure - LV diastolic pressure) at >60 mmHg. Ventricular arrhythmias were treated with lidocaine (50-100 mg, i.v.) and amiodarone (50-150 mg, i.v.), as needed. Twelve animals died during the infarction procedure due to refractory ventricular fibrillation. The remaining animals were followed for clinical signs of heart failure (tachypnea, lethargy, anorexia), and serial transthoracic echocardiography was performed to detect left ventricular dilatation and mitral regurgitation (MR).

After a mean of 7 ± 1 weeks, the animals were returned to the cardiac catheterization laboratory for recording of hemodynamic, TEE, and marker data. Mitral regurgitation was graded by an experienced echocardiographer (D.L.), based on regurgitant jet extent and width, as none (0), trace (+0.5), mild (+1), moderate (+2), moderate-severe (+3), or severe (+4). Of the 20 remaining animals, eight developed only trace to mild MR. Twelve animals developed moderate or more MR, and these comprised the group studied in the present report.

All animals received humane care in compliance with the *Principles of Laboratory Animal Care* formulated by the National Society for Medical Research and the *Guide for Care and Use of Laboratory Animals* prepared by the National Academy of Sciences and published by the National Institutes of Health (DHEW NIHG publication 85-23, revised 1985). This study was approved by the Stanford University Medical School Laboratory Research Animal Review committee and conducted according to Stanford University policy.

Data acquisition

Images were acquired with each animal in the right lateral position using a biplane videofluoroscopy system (Philips Medical Systems, North America Company, Pleasanton, CA, USA). Data from two radi-

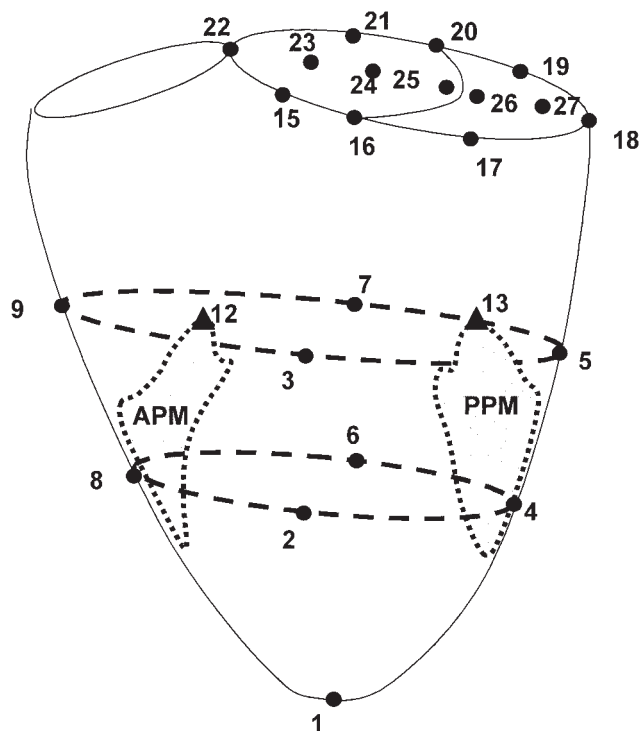


Figure 1: Schematic of marker array used in this study. Markers were placed on the left ventricle, papillary muscle tips, leaflets, and annulus. APM: Anterior papillary muscle; PPM: Posterior papillary muscle.

ographic views were digitized and merged to yield 3-D coordinates for each of the radiopaque markers every 16.7 ms using custom-designed software. Ascending aortic pressure, left ventricular pressure (LVP), and ECG voltage signals were digitized and recorded simultaneously during marker data acquisition.

Data analysis

Hemodynamics and cardiac cycle timing

Three consecutive steady-state beats before myocardial infarction were averaged and defined as 'Baseline' data for each animal. Similarly, at the follow up study, three beats were averaged and termed 'CIMR' data. During each cardiac cycle, end-systole (ES) was defined as the time of the videofluoroscopic frame containing the point of peak negative rate of LVP fall ($-dP/dt$), and end-diastole (ED) as the videofluoroscopic frame prior to the upstroke of the LVP curve. Instantaneous left ventricular volume was calculated from the positions of the epicardial left ventricular markers and annular markers using a space-filling multiple tetrahedral volume method for each frame (i.e. every 16.7 ms).

Mitral annular geometry

The end-systolic septal-lateral (S-L) diameter of the annulus was calculated as the distance in 3-D space between the two markers placed in the middle of the septal and lateral mitral annulus, respectively (#22 and 18; Fig. 1). The commissure-commissure (C-C) diameter was calculated as the distance between the two annular commissural markers (#16 and 20; Fig. 1).

Papillary muscle geometry

To characterize subvalvular geometry, the end-systolic distance in 3-D space from each papillary muscle tip (#12, #13; Fig. 1) to the mid-septal annulus (#22), was calculated. Similarly, the end-systolic distances from the anterior papillary muscle tip to the anterior commissure (#12-#16) and from the posterior papillary muscle tip to the posterior commissure (#13-#20) were computed.

Leaflet radii of curvature

Mitral leaflet ROC at end-systole were measured along the midline of each leaflet using the marker coordinates along the lateral and apical axes. The 3-D coordinates of the markers were projected onto a plane containing the mid-septal annular marker (#22), the mid-lateral annular marker (#18) and the left ventricular apex (#1). The chord joining the mid-septal and mid-lateral annular markers defined the septal-lateral axis, with the apical-basal axis directed perpendicular to the annular plane. The central meridian of the ante-

rior leaflet had a sigmoid shape, convex to the left ventricle proximally (near the annulus) and concave to the left ventricle distally (near the leaflet edge) (Fig. 2). The central meridian of the posterior leaflet was concave to the left ventricle (Fig. 2). Three markers were used to define the ROC of each of these curves. Each marker triad defined a unique circumscribed circle, the radius of which was the ROC. For example, the ROC of the proximal anterior leaflet was computed from the lateral and apical coordinates of markers #22, 23, and 24.

Effective leaflet length

Effective leaflet length was calculated as the 3-D distance from the annular marker at the base of each leaflet to the leaflet edge (#22 to 25 for the AML; #18 to 26 for the PML). In Figure 2, the effective leaflet length would be the distance from the base of each leaflet, at the top of the figure, to the edge of each leaflet, at the bottom of the figure.

Statistical analysis

All data were reported as mean \pm SD. Comparisons

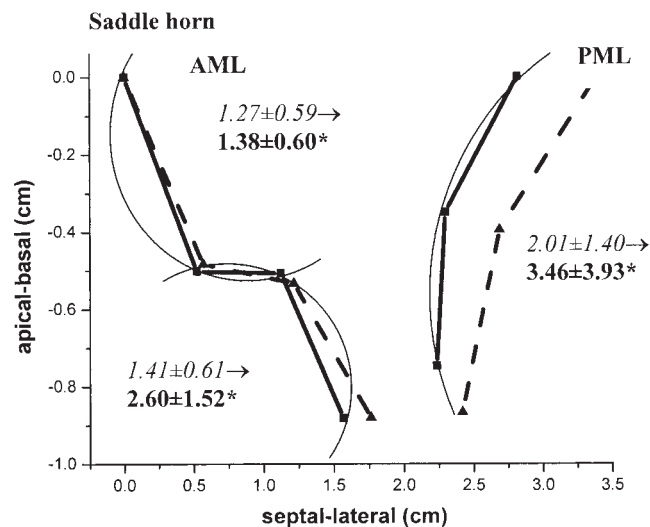


Figure 2: Two-dimensional plot of group mean end-systolic leaflet marker position projected onto the lateral-apical plane showing mid-line section of leaflet shape at Baseline (solid lines and squares) and after CIMR (dotted lines and triangles). The saddlehorn, or mid-septal annulus, is shown for reference. Arcs schematically represent portions of circumscribed circles used to calculate leaflet radii of curvature for Baseline (above in italics) and CIMR (below in bold). The anterior mitral leaflet shows a compound curvature. CIMR is associated with increased radii of curvature for both the anterior and posterior leaflets. The leaflets do not appear to be in contact, even in the normal competent valve, as the markers are not placed on the very edges of the leaflets. AML: Anterior mitral leaflet; PML: Posterior mitral leaflet. * $p < 0.05$ versus Baseline.

Table I: Hemodynamic data.

Parameter	Baseline	CIMR
MR (grade 0-4+)	0.6 ± 0.5	2.5 ± 0.7*
LV dP/dt _{max} (mmHg/s)	1,837 ± 683	1163 ± 482*
LVP _{max} (mmHg)	96 ± 14	75 ± 20*
EDV (ml)	107 ± 20	145 ± 20*
LVEDP (mmHg)	17 ± 3	21 ± 4*

*p < 0.05 versus Baseline.

CIMR: Chronic ischemic mitral regurgitation; dP/dt_{max}: Maximum of first derivative of pressure versus time; EDV: End-diastolic volume; LVEDP: Left ventricular pressure at end-diastole; LVP_{max}: Maximum left ventricular pressure; MR: Mitral regurgitation.

between Baseline and CIMR conditions were made with Student's *t*-test for paired observations. Hemodynamic and geometric data from the baseline and chronic studies were entered into a stepwise multivariable regression model to identify significant predictors of mitral leaflet ROC (SPSS, v.10.1).

Results

Group mean hemodynamic data at baseline and after CIMR are summarized in Table I. Maximum left ventricular dP/dt and maximum LVP decreased with CIMR, while MR, left ventricular end-diastolic pressure and left ventricular end-diastolic volume all increased.

Mitral annular dimensions and papillary muscle positions at end-systole are summarized in Table II. With CIMR, the annulus dilated in both the S-L and C-C dimensions. The distances from each papillary muscle tip to the saddle horn also increased. The distance between the anterior papillary muscle tip and the anterior commissure increased, but the distance from the posterior papillary muscle tip to the posterior commissure did not change.

Group mean data on leaflet ROC and length at Baseline and with CIMR are summarized in Table III. The proximal and distal anterior leaflet ROC both

increased, coincident with an increase in the effective length of the leaflet from base to edge. Similarly, the posterior mitral leaflet ROC increased, associated with an increase in the effective length of the posterior leaflet. These results are illustrated graphically in Figure 2.

In the stepwise multivariable regression analysis, S-L dimension was the only independent predictor of the proximal AML curve ($\beta = 0.63$). S-L annular diameter and the distance from the anterior papillary muscle tip to the anterior commissure were roughly equally strong predictors of the ROC of the distal AML curve ($\beta = 0.48$ and 0.45 , respectively), and the distance from the posterior papillary muscle tip to the saddle horn was the best predictor of the PML ROC ($\beta = 0.37$).

Discussion

Curvature is a fundamental component of the shape - and thereby stress - on the mitral leaflet, and is therefore an important element of normal valve function. The new in-vivo data reported herein support four conclusions: (i) At end-systole, the anterior leaflet has a sigmoid shape; (ii) the ROC of the curves of both the anterior and posterior leaflets increase with CIMR; (iii) changes in ROC that occur in CIMR are predicted by annular and subvalvular geometry; and (iv) CIMR is

Table II: Annular and subvalvular geometry.

Parameter	Baseline	CIMR
S-L annular diameter (cm)	2.83 ± 0.28	3.23 ± 0.41*
C-C annular diameter (cm)	3.53 ± 0.29	4.06 ± 0.36*
APM to saddle horn (cm)	4.51 ± 0.49	4.71 ± 0.49*
PPM to saddle horn (cm)	5.13 ± 0.97	5.62 ± 0.97*
ACOM to APM (cm)	3.49 ± 0.53	3.56 ± 0.51*
PCOM to PPM (cm)	3.94 ± 1.00	3.92 ± 1.23

*p < 0.05 versus Baseline.

ACOM: Anterior commissure; APM: Anterior papillary muscle; C-C: Commissure-commissure; PCOM: Posterior commissure; PPM: Posterior papillary muscle; S-L: Septal-lateral.

Table III: Leaflet radii of curvature (ROC) and effective length.

Parameter	Baseline	CIMR
AML proximal ROC (cm)	1.27 ± 0.59	1.38 ± 0.60*
AML distal ROC (cm)	1.41 ± 0.61	2.60 ± 1.52*
PML ROC (cm)	2.01 ± 1.40	3.46 ± 3.93*
AML length (cm)	2.06 ± 0.54	2.20 ± 0.46*
PML length (cm)	1.16 ± 0.23	1.24 ± 0.27*

*p <0.05 versus Baseline.

AML: Anterior mitral leaflet; PML: Posterior mitral leaflet; ROC: Radii of curvature.

associated with increases in the effective length of the leaflets.

Leaflet geometry

Existing finite element and other mathematical models of the mitral valve during systole consider both leaflets as passive membranes with an elliptical shape (1-3,6). When observing through the left atrium in an arrested heart, cardiac surgeons realize that the leaflets of a competent, normal mitral valve bulge toward the atrium when the left ventricle is filled with fluid. Similar shapes have been derived from casts of excised hearts (4). Myocardial marker technology allows the spatial and temporal resolution to delineate precisely the in-vivo leaflet shape and to quantify curvature in the beating heart, as well as the ability to track specific loci on the leaflets in four dimensions to assess changes due to CIMR. It was found that the anterior leaflet in vivo adopts a compound shape at end systole, as illustrated in Figure 2 and previously described by Karlsson et al. (11), with a proximal curve convex to the left ventricle and a distal curve concave to the left ventricle. The proximal bend, which is maintained convex to the ventricle even under systolic pressures, is likely maintained by the interplay of forces between the annulus, leaflet, and second-order chordae which insert close to the annulus (9,11). Previous reports of mitral valve geometry have described a direction of leaflet curvature at valve closure (9-11,17), but the present analysis further defines leaflet shape by quantifying the radius of the curve.

The posterior leaflet, in contrast to the anterior, exhibits a single, flatter curve, concave to the left ventricle at end-systole (Fig. 2). This finding again supports the cinefluoroscopy studies of Karlsson et al. (11), as well as those by Sovak et al. (18) and Levine et al. (17), using 3-D echo, who reported a convex curvature to the posterior leaflet when the valve was closed.

Changes in geometry with CIMR

Inferior myocardial infarction and CIMR caused, in

the present study and in others (12,14), not only global ventricular dilation but also changes in annular and papillary muscle geometry. In particular, the distances from the papillary muscle tips to the mid-septal annulus, or saddle horn (sometimes called the papillary muscle tethering distance (12)), were increased. Also, the relationship between the anterior papillary muscle tip and the anterior commissure changed - something which previously was associated with loss of valve competence in acute ischemic MR (19). In finite element models, such changes in valve geometry significantly increase leaflet stress (5,20).

With CIMR, the radii of both curves of the anterior leaflet and the curve of the posterior leaflet were increased. It follows from the law of Laplace that the increases in curvature observed here will tend to accentuate leaflet stress in these thin membranes. The observed 'flattening' of the curves is consistent with increased effective length of the leaflets between the annulus and the leaflet leading edges. This 'unfurling' of redundant leaflet tissue has been described in ex-vivo anatomical (21) and in-vivo functional (15) studies of the mitral apparatus. Lai et al., in the present authors' laboratory, reported that during acute circumflex ischemia, this leaflet lengthening may be a compensatory mechanism for the valve to limit the size of the effective regurgitant orifice (15). The findings of the present study indicate, however, that such compensation comes at a price, which is increased leaflet ROC that would actually be expected to increase leaflet stress. In addition to unfurling, effective leaflet length could also be partly achieved through stretching of the leaflet tissue. Consistent with the present findings and the finite element models showing increased leaflet stress after annular and papillary muscle remodeling, Quick et al. demonstrated up-regulation of collagen synthesis in response to increased stress in the anterior leaflets of sheep with CIMR (8). While increased leaflet thickness may normalize stress, computer models indicate that it may also decrease leaflet mobility, eventually exacerbating malcoaptation, increasing MR, and

producing further ventricular remodeling in a self-serving viscous cycle (7,8).

Clinical implications

The greater leaflet ROC associated with CIMR favor increased leaflet stress, and may play a role in a feedback loop between mitral leaflet tissue and left ventricular remodeling. This may help to explain the old adage, 'MR begets MR', and should spur clinicians to recommend mitral repair earlier in the natural history of CIMR before excessive leaflet tissue degeneration and/or thickening or valvular-ventricular remodeling occur. Further, as changes in both annular and papillary muscle geometry determine leaflet ROC, subvalvular adjuncts to ring annuloplasty such as papillary muscle relocation (22), should be explored in order to normalize leaflet stress after mitral repair. In the future, computer models, taking into account experimentally measured in-vivo annular, papillary muscle and leaflet 3-D geometry will hopefully prove valuable in the design of custom-tailored mitral repair procedures and techniques which will minimize leaflet stresses.

Study limitations

The present study was performed in an ovine model of CIMR, and several limitations must be noted. First, leaflet curvature was studied only at the midline region and only during end-systole. Using a marker array with more midline leaflet markers, Karlsson et al. (11) noted that the same leaflet shapes (compound shape for the anterior leaflet and convex to the left ventricle for the posterior leaflet) were maintained throughout the latter half of systole. Leaflet shape, qualitatively described in diastole by Karlsson et al., features more variability and flatter leaflet shapes (11) (with the leaflet ROC rapidly approaching infinity), making quantitative description of leaflet curvature during diastole difficult to interpret. The determination of leaflet shape at more sites, or in different directions, would require many more markers than the array used in the present study. The law of Laplace applies strictly only to cylinders and spheres; thus, stress alterations due to changes in leaflet shape are approximations at best. The myocardial marker method provides submillimeter spatial resolution every 16.7 ms, but requires markers to be sutured to intracardiac structures; hence it is possible - though unlikely, due to their small size - that the markers interfered with leaflet geometry and motion.

In conclusion, the end-systolic 3-D shape of the mitral leaflets before and after development of CIMR was analyzed in an ovine model. With the valve closed, the anterior leaflet has a compound shape, while the pos-

terior leaflet has a single curve convex to the left ventricle. CIMR increases the ROC of both the anterior and posterior leaflets, which in turn would be expected to increase leaflet stress. Both annular and subvalvular geometry influence leaflet curvature, and septal-lateral annular diameter and posterior papillary muscle tethering distance should be considered as potential targets during mitral repair for CIMR to reduce leaflet stress. These novel quantitative in-vivo data are now available for modification of finite element models, and for comparison to finite element model output.

Acknowledgements

The authors gratefully acknowledge the superb technical assistance of Carol W. Mead and Maggie Brophy in the conduct of these experiments and analysis of the data. The studies were supported by grants HL-29589 and HL-67025 from the National Heart, Lung and Blood Institute. Drs. Tibayan and Rodriguez are Carl and Leah McConnell Cardiovascular Surgical Research Fellows. Dr. Tibayan was supported by NHLBI Individual Research Service Award HL-67563. Dr. Rodriguez was supported by Grant HL67025-01S1 from the NHLBI and was a recipient of the American College of Surgeons Resident Research Scholarship Award.

References

1. Mazumdar J, Hearn TC. Mathematical analysis of mitral valve leaflets. *J Biomech* 1978;11:291-296
2. Arts T, Meerbaum S, Reneman R, Corday E. Stresses in the closed mitral valve: A model study. *J Biomech* 1983;16:539-547
3. Miller GE, Marcotte H. Computer simulation of human mitral valve mechanics and motion. *Comput Biol Med* 1987;17:305-319
4. Kunzelman KS, Cochran RP, Chuong C, Ring WS, Verrier ED, Eberhart RD. Finite element analysis of the mitral valve. *J Heart Valve Dis* 1993;2:326-340
5. Cochran RP, Kunzelman KS. Effect of papillary muscle position on mitral valve function: Relationship to homografts. *Ann Thorac Surg* 1998; 66(6 Suppl.):S155-S161
6. Salgo IS, Gorman JH, III, Gorman RC, et al. Effect of annular shape on leaflet curvature in reducing mitral leaflet stress. *Circulation* 2002;106:711-717
7. Kunzelman KS, Quick DW, Cochran RP. Altered collagen concentration in mitral valve leaflets: Biochemical and finite element analysis. *Ann Thorac Surg* 1998; 66(6 Suppl.):S198-S205
8. Quick DW, Kunzelman KS, Kneebone JM, Cochran RP. Collagen synthesis is upregulated in mitral valves subjected to altered stress. *Am Soc Artif Intern Organs J* 1997;43:181-186
9. Messas E, Guerrero JL, Handschumacher MD, et al.

- Chordal cutting: A new therapeutic approach for ischemic mitral regurgitation. *Circulation* 2001;104:1958-1963
10. Pohost GM, Dinsmore RE, Rubenstein JJ, et al. The echocardiogram of the anterior leaflet of the mitral valve. Correlation with hemodynamic and cinerentgenographic studies in dogs. *Circulation* 1975;51:88-97
 11. Karlsson MO, Glasson JR, Bolger AF, et al. Mitral valve opening in the ovine heart. *Am J Physiol* 1998;274(2 Pt.2):H552-H563
 12. Otsuji Y, Handschumacher MD, Liel-Cohen N, et al. Mechanism of ischemic mitral regurgitation with segmental left ventricular dysfunction: Three-dimensional echocardiographic studies in models of acute and chronic progressive regurgitation. *J Am Coll Cardiol* 2001;37:641-648
 13. Tibayan FA, Rodriguez F, Zasio MK, et al. Geometric distortions of the mitral valvular-ventricular complex in chronic ischemic mitral regurgitation. *Circulation* 2003;108(Suppl.1):II116-II121
 14. Yiu SF, Enriquez-Sarano M, Tribouilloy C, Seward JB, Tajik AJ. Determinants of the degree of functional mitral regurgitation in patients with systolic left ventricular dysfunction: A quantitative clinical study. *Circulation* 2000;102:1400-1406
 15. Lai DT, Tibayan FA, Timek TA, et al. Three-dimensional in-vivo dimensions of 'He's triangle' during acute left ventricular ischemia. *J Heart Valve Dis* 2001;10:767-773
 16. Llaneras MR, Nance ML, Streicher JT, et al. Pathogenesis of ischemic mitral insufficiency. *J Thorac Cardiovasc Surg* 1993;105:439-442
 17. Levine RA, Handschumacher MD, Sanfilippo AJ, et al. Three-dimensional echocardiographic reconstruction of the mitral valve, with implications for the diagnosis of mitral valve prolapse. *Circulation* 1989;80:589-598
 18. Sovak M, Lynch PR, Stewart GH. Movement of the mitral valve and its correlation with the first heart sound. Selective valvular visualization and high-speed cineradiography in intact dogs. *Invest Radiol* 1973;8:150-155
 19. Dagum P, Timek TA, Green GR, et al. Coordinate-free analysis of mitral valve dynamics in normal and ischemic hearts. *Circulation* 2000;102(19 Suppl.3):III62-III69
 20. Kunzelman KS, Reimink MS, Cochran RP. Annular dilatation increases stress in the mitral valve and delays coaptation: A finite element computer model. *Cardiovasc Surg* 1997;5:427-434
 21. He S, Weston MW, Lemmon J, Jensen M, Levine RA, Yoganathan AP. Geometric distribution of chordae tendineae: An important anatomic feature in mitral valve function. *J Heart Valve Dis* 2000;9:495-501
 22. Kron IL, Green GR, Cope JT. Surgical relocation of the posterior papillary muscle in chronic ischemic mitral regurgitation. *Ann Thorac Surg* 2002;74:600-601

Meeting discussion

DR. KARYN KUNZELMAN (Madison, WI, USA): I have a comment and a question. The comment is that our data on finite element models for papillary muscle displacement tend to agree in general in terms of leaflet flattening. My question is related to those animals that did not have progression of MR. The sheep is a very difficult model. We had several with initial MR at the time of operation that did not progress, and our first thought was that the model did not work. But there turned out to be significant changes in the leaflet collagen, procollagen, heat shock, so that on analysis it appeared that the leaflets were tending to heal. Have you studied - or will you study - also those animals that did not progress to MR, to see if there are any changes in parameters that would lead towards a decrease in MR?

DR. FREDERICK A. TIBAYAN (Stanford, CA, USA): That analysis has been done, but the data were not presented here due to time constraints. In the animals that survived for seven weeks but did not develop significant MR, there was a tendency towards increased leaflet radii of curvature, but the change was not statistically significant. This may have been due to a lack of power in the study, as the numbers were low and there was obvious biological variability. But I don't doubt that some biochemical changes may be occurring in those leaflets.

DR. IVAN VESELY (Cleveland, OH, USA): Did you put your markers on the ventricular or on the atrial surface of the leaflets?

DR. TIBAYAN: They were placed on the atrial surface.

DR. VESELY: So you're quite confident that that inverse curvature from base to the central portion is real, and not caused by any surface irregularities?

DR. TIBAYAN: Well, that's possible, but the size of the markers is probably not big enough, if you consider the overall contours, to really change the shape of the leaflet. I think there may be small changes, but probably not too great.